

# Entanglement Dimensionality of Continuous Variable States From Phase-Space Quasi-Probabilities

Shuheng Liu,<sup>1,2</sup> Jiajie Guo,<sup>1</sup> Matteo Fadel,<sup>3,\*</sup> Qiongyi He,<sup>1,4,5,†</sup> Marcus Huber,<sup>2,6,‡</sup> and Giuseppe Vitagliano<sup>2,§</sup>

<sup>1</sup>*State Key Laboratory for Mesoscopic Physics, School of Physics,  
Frontiers Science Center for Nano-optoelectronics, Peking University, Beijing 100871, China*

<sup>2</sup>*Vienna Center for Quantum Science and Technology, Atominstitut, TU Wien, 1020 Vienna, Austria*

<sup>3</sup>*Department of Physics, ETH Zürich, 8093 Zürich, Switzerland*

<sup>4</sup>*Collaborative Innovation Center of Extreme Optics, Shanxi University, Taiyuan, Shanxi 030006, China*

<sup>5</sup>*Hefei National Laboratory, Hefei 230088, China*

<sup>6</sup>*Institute for Quantum Optics and Quantum Information (IQOQI), Austrian Academy of Sciences, 1090 Vienna, Austria*

The dimensionality of entanglement is a core tenet of quantum information processing, especially quantum communication and computation. While it is natural to think of this dimensionality in finite dimensional systems, many of the implementations harnessing high Schmidt numbers are actually based on discretising the observables of continuous variable systems. For those instances, a core question is whether directly utilizing the toolbox of continuous variable quantum information processing leads to better and more robust characterisations of entanglement dimensionality in infinite dimensional systems. We affirmatively answer this question by introducing Schmidt number witnesses for CV systems, based directly on covariances of infinite dimensional Bloch operators that are readily accessible in experiments. We show that the direct estimation leads to increased robustness and versatility compared to first discretising the system and using canonical discrete variable techniques, which provides strong motivation for further developments of genuine CV methods for the characterization of entanglement dimensionality, as well as for their implementation in experiments.

**Introduction.—** Significant effort has been devoted to characterizing entanglement in continuous-variable (CV) quantum systems [1, 2] in experimentally accessible ways, despite the complication posed by the formally infinite-dimensional Hilbert space. Most prominently, conditions on the covariance matrix of the quadratures have been investigated [3, 4], as well as approaches based on the moment of the mode operators [5–7]. The former method has the advantage of being more readily applicable also to multi-mode systems [8, 9] and to characterize genuine multipartite entanglement [10, 11]. Other approaches are instead based on phase-space quasi-probability distributions, which can be seen as arising from correlations of continuous-variable *Local Orthogonal Observables* (CVLOOs), such as displacements or displaced-parity operators [12, 13].

From these methods, it is also possible to quantify entanglement by bounding entanglement monotones, such as the entanglement of formation or the entanglement negativity [10, 13–16]. However, these bounds are not directly applicable to the so-called *entanglement dimensionality*, which is an important quantifier of the effective dimension that is required to describe the observed correlations. For a bipartite system in the pure state  $|\psi\rangle = \sum_{k=1}^r \sqrt{\lambda_k} |u_k\rangle |v_k\rangle$ , this is typically quantified through the Schmidt rank  $SN(\psi)$  that is defined as the number of nonzero Schmidt coefficients  $\lambda_k$ , i.e., the rank of the single-particle reduced density matrix. This entanglement monotone can be extended to mixed states by considering a worst-case scenario over all decompositions [17]:

$$SN(\varrho) := \inf_{\mathcal{D}(\varrho)} \max_{|\psi_i\rangle \in \mathcal{D}(\varrho)} SN(\psi_i), \quad (1)$$

where the minimization is over all pure-state decompositions  $\mathcal{D}(\varrho) = \{p_i, |\psi_i\rangle\} : \varrho = \sum_i p_i |\psi_i\rangle\langle\psi_i|$ . This defines the so-called

*Schmidt number* for bipartite density matrices, a quantity that plays a central role in various single-shot tasks and stands as one of the few entanglement measures linked to quantum computational advantage [18–20]. Crucially, it also serves as an indicator for accessing the enhanced capabilities offered exclusively by higher-dimensional quantum systems [21–23].

Certifying the effective dimension of a system is particularly important for platforms that are formally described by an infinite-dimensional Hilbert space, which can never be fully accessed or controlled in practice due to the fundamental limitation of finite experimental resources (e.g. bounded energy). In particular, although CV platforms have become one of the leading architectures for quantum information tasks, generating and precisely controlling states of effectively high dimensionality, such as those exhibiting entanglement across many Fock states, remains highly nontrivial. Numerous recent experiments already realize and exploit high-dimensional entanglement in CV degrees of freedom by discretizing spatial, temporal, or spectral modes and working within finite subspaces [24–32], which further motivates robust Schmidt-number certification in CV settings. Various criteria to characterize entanglement dimensionality in CV systems have been developed [33, 34], e.g. based on the covariance matrix of quadratures; however, these are far from exhaustive and, crucially, are often outperformed in practice by truncation- and fidelity-based approaches, particularly in the non-Gaussian regime. The latter are in fact the most common methods employed in experiments, where the fidelity to a finite-dimensional truncation of the state is considered [35].

We consider here a bipartite system, where each party consists of a CV mode described by the bosonic operators  $(\hat{a}_k^\dagger, \hat{a}_k)$  obeying the canonical commutation relation  $[\hat{a}_j, \hat{a}_k^\dagger] = \delta_{jk} \hat{1}$  [36]. As we mentioned, a typical way of quantifying the

entanglement dimensionality is via the monotone in Eq. (1). Even though this definition applies to both DV and CV systems, in the latter case note that even very small non-zero Schmidt coefficients contribute to it, and for many relevant states the Schmidt number is in fact unbounded. For instance, an ideal two-mode squeezed vacuum state, even with arbitrarily small nonzero squeezing, possesses an infinite Schmidt number. At the same time, in practical implementations, the experimental limitations, due to noise and also limited detection capabilities render the entanglement dimensionality effectively finite [37]. Because of that, this quantity especially attracts a lot of interest in experiments that aim at the certification of entanglement. Previous methods, however, truncated the infinite CV space to compute Schmidt numbers in the effectively discretised spaces using traditional methods for finite dimensional systems. While this is technically easy to do on paper, it does not leverage the sophisticated measurement techniques that are specifically suited for CV systems. Our work aims at filling this gap by presenting new entanglement dimensionality criteria based on the available CV toolbox.

**Theoretical methods.**—The canonical fidelity-based witness for discrete systems are given in terms of an upper-bound to the fidelity with respect to a target state  $|\Psi_T\rangle = \sum_k \sqrt{\lambda_k} |kk\rangle$  ( $\lambda_k$  ordered non-increasingly), that typically corresponds to the ideal (high-dimensional entangled) preparation expected in an experiment. More precisely, the following upper-bound

$$\mathcal{F}(\varrho, |\Psi_T\rangle) \leq \sum_{k=1}^r \lambda_k, \quad (2)$$

holds for all density matrices  $\varrho$  with Schmidt number upper-bounded by  $r$ , where the fidelity (to a pure state) is defined as  $\mathcal{F}(\varrho, |\Psi_T\rangle) = \langle \Psi_T | \varrho | \Psi_T \rangle$ .

As it is known that not every entangled (or high-dimensional) state can be witnessed by a fidelity type witness [38], there are of course more sophisticated methods that have been developed. From  $k$ -positive maps [17] to covariances of operator expectation values [39], that can even reveal PPT entangled states of high-dimension [40–42].

Importantly, no method that makes use of a genuinely CV characterization of the state in order to certify the Schmidt number, e.g., through the estimation of phase-space quasi-probability distributions, was available. This is what we are going to develop in the following.

Here, building upon the finite-dimensional framework [39], we consider a set of CVLOOs, i.e., an *orthonormal* set of operators  $\{Q(\alpha)\}_{\alpha \in \mathbb{C}}$ , where  $\alpha \in \mathbb{C}$ , that are such that they span the observables' space of a bosonic mode. Orthonormality is given by the condition

$$\text{tr}(Q(\alpha) Q(\beta)) = \delta^{(2)}(\alpha - \beta). \quad (3)$$

For example, the displacement operator  $D(\alpha) = e^{\alpha \hat{a}^\dagger - \alpha^* \hat{a}}$ , where  $\alpha \in \mathbb{C}$ , defines the characteristic function  $\chi_\varrho(\alpha) = \text{tr}(D(\alpha)\varrho)$ , i.e., it provides a full description of the density matrix and can be used to construct examples of CVLOOs. One

simple way is to consider its hermitian and normalized version, which is given by  $Q(\alpha) = \frac{1+i}{2\sqrt{\pi}} D(\alpha) + \frac{1-i}{2\sqrt{\pi}} D^\dagger(\alpha)$ . Similarly, from the definition of the Wigner function  $W_\varrho(\alpha) = \frac{2}{\pi} \text{tr}(\varrho D(\alpha) \Pi D^\dagger(\alpha))$  where  $\Pi = (-1)^{a^\dagger a}$  is the parity operator [44–46] we see that CVLOOs can be constructed from the displaced parity. In general CVLOOs can be transformed into each other via orthogonal kernels  $Q'(\beta) = \int_{\mathbb{C}} O(\beta, \alpha) Q(\alpha) d^2\alpha$  with  $O(\beta, \alpha) = \text{tr}(Q'(\beta) Q(\alpha))$ . This transformation satisfies  $\int_{\mathbb{C}} O^\dagger(\beta, \alpha) O(\beta', \alpha) d^2\alpha = \delta^{(2)}(\beta - \beta')$ . For  $M$  modes, one way to construct a CVLOO is by taking tensor products of the single mode ones, i.e.,  $Q(\alpha) = Q(\alpha_1) \otimes \cdots \otimes Q(\alpha_M)$ , where  $\alpha = (\alpha_1, \dots, \alpha_M)$ .

Estimation of entanglement with measurements of these CVLOOs has been already investigated to some extent, by developing entanglement witnesses that mimic the so-called Computable Cross-Norm and Realignment (CCNR) criterion [13, 47, 48], or also the PPT criterion [48]. In particular, from CVLOOs, one can find bounds to the trace norms  $\|\mathcal{R}(\varrho)\|$  and  $\|\mathcal{T}_A(\varrho)\|$ , where  $\mathcal{R}$  and  $\mathcal{T}_A$  are the realignment and partial transposition map respectively. Then, one can detect entanglement from violations of the criteria  $\|\mathcal{R}(\varrho)\| \leq 1$  and  $\|\mathcal{T}_A(\varrho)\| \leq 1$  respectively, which also detect in general different states, with the exception of two-mode Gaussian states, where the latter criterion is both necessary and sufficient.

For two modes, weaker versions of these witnesses can be cast in the form

$$\begin{aligned} \int_{\mathbb{C}} \langle O_A(\alpha) \otimes \tilde{O}_B(\alpha) \rangle d^2\alpha &\leq \|\mathcal{T}_A(\varrho)\| \leq 1, \\ \int_{\mathbb{C}} |Q_A(\alpha) \otimes Q_B(\alpha)| d^2\alpha &\leq \|\mathcal{R}(\varrho)\| \leq 1, \end{aligned} \quad (4)$$

where  $Q_A(\alpha)$  and  $Q_B(\alpha)$  are two CVLOOs, while  $O_A(\alpha)$  and  $\tilde{O}_B(\alpha)$  are similar operators, with the normalization satisfying  $s \text{tr}(O_A(\alpha) O_A(\beta)) = (2-s) \text{tr}(\tilde{O}_B(\alpha) \tilde{O}_B(\beta)) = \delta^{(2)}(\alpha - \beta)$  where  $0 < s < 2$ . See also End Matter for some details. Typical choices of CVLOOs considered are constructed from the hermitian part of the displacement operator [13, 47], that we also consider in the following, and the displaced parity [48]. For obtaining a witness equivalent to the CCNR criterion one has to pick the two optimal CVLOOs that arise from the operator-Schmidt decomposition of the density matrix, and are generally different than these. However, the operators considered in Refs. [13, 47, 48] are  $Q(f(\alpha))$  with  $\det J_f = \pm 1$ , where  $[J_f]_{kl} = \partial[f(\alpha)]_k / \partial \alpha_l$  is the Jacobian of the transformation and  $\alpha_1 = \text{Re } \alpha$ ,  $\alpha_2 = \text{Im } \alpha$ . Substituting these CVLOOs in Eq. (4) leads to a witness equivalent to the CCNR for symmetric Gaussian states (however, not necessarily optimal for generic two-mode states).

**New criteria.**—Next, we extend those results by both generalizing these bounds to detect the entanglement dimensionality, and by considering another criterion containing non-linear terms, that make it strictly stronger than the CCNR. (See fig. 1 for a conceptual figure, clarifying how our new criteria are related to existing works.) In doing this, we also improve the detection of entanglement dimensionality in CV systems as compared to truncating their Hilbert space at some

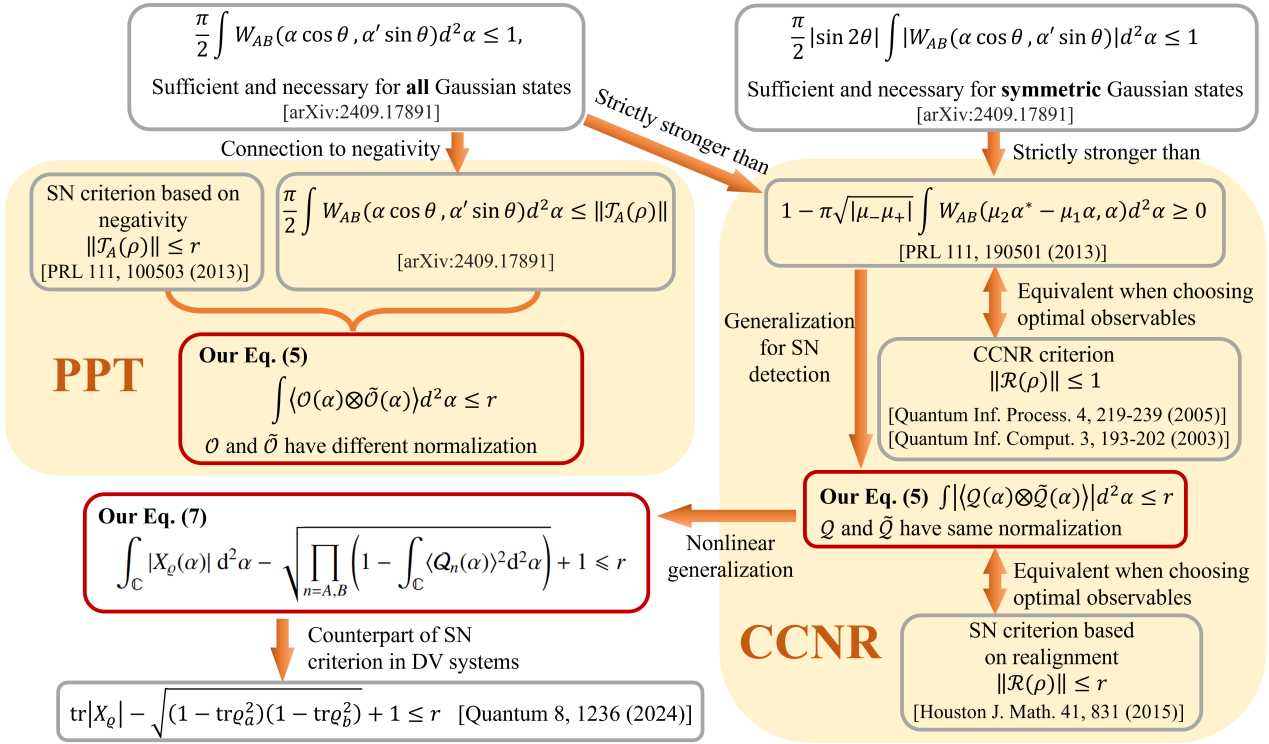


FIG. 1. Conceptual map illustrating the relationships between the criteria introduced in this work (red boxes) and criteria from the literature (gray boxes).

finite dimension. Thus, we find that a first way to extend Eq. (4) to detect the Schmidt number would be to use the inequalities  $\|\mathcal{R}(\rho)\| \leq r$  and  $\|\mathcal{T}_A(\rho)\| \leq r$ , which hold for all states with Schmidt number bounded from above by a given  $r$  [49–51], obtaining an expression of the form

$$\int_{\mathbb{C}} \langle \mathcal{O}_A(\alpha) \otimes \tilde{\mathcal{O}}_B(\alpha) \rangle d^2 \alpha \leq r, \quad (5)$$

where again, as in Eq. (4),  $\mathcal{O}_A(\alpha)$  and  $\tilde{\mathcal{O}}_B(\alpha)$  are operators similar to CVLOOs, but potentially with a different normalization. Hence, this approach already provides a witness of the Schmidt number based on correlations between CVLOOs. In what follows we derive another condition that is strictly stronger than a bound on the realigned density matrix and can potentially detect a wider set of states than the bounds in Eq. (5).

Once again, we consider for simplicity a bipartite system with one bosonic mode in each of the two parties, but our results can be easily extended to the more general scenario of  $(M + N)$ -mode systems. This criterion is based on cross-covariances between two observables, which are defined as  $\Gamma_{\rho}(Q_A, Q_B) := \langle Q_A \otimes Q_B \rangle_{\rho} - \langle Q_A \rangle_{\rho} \langle Q_B \rangle_{\rho}$ . In particular, we consider a pair of CVLOOs for the two parties and align their phase-space variable (which can be done via a simple local change of CVLOO, e.g., corresponding to a canonical transformation) so to consider the following covariances:

$$X_{\rho}(\alpha) := \Gamma_{\rho}(Q_A(\alpha), Q_B(\alpha)), \quad (6)$$

where  $\{Q_A(\alpha)\}$  and  $\{Q_B(\alpha)\}$  are two suitably chosen CVLOOs [52]. Specifically, we mostly restrict to bases of the form  $Q(f(\alpha)) = \frac{1+i}{2\sqrt{\pi}} D(f(\alpha)) + \frac{1-i}{2\sqrt{\pi}} D^{\dagger}(f(\alpha))$  with additional phase-space transformations such that  $\det J_{f_A} \det J_{f_B} = \pm 1$  where again  $J_f$  is the Jacobian matrix. This is because in this way our entanglement condition can be evaluated in a simpler way, by just measuring the bipartite characteristic function along a two-dimensional plane, as we are going to discuss in more detail in the following.

Based on these quantities, we can prove that for any state with Schmidt number not larger than a given  $r$ , the following inequality holds

$$\int_{\mathbb{C}} |X_{\rho}(\alpha)| d^2 \alpha - \sqrt{\prod_{n=A,B} \left( 1 - \int_{\mathbb{C}} \langle Q_n(\alpha) \rangle^2 d^2 \alpha \right)} + 1 \leq r. \quad (7)$$

This condition has some similarities with Eq. (5). However, it contains additional terms that are nonlinear in the quantum state and in some cases provides a bound that is strictly stronger than the CCNR criterion [47].

We can recover an expression like that in Eq. (5) by further approximating the left-hand side of Eq. (7). In particular, this way we can find a linear witness criterion similar to the CCNR and a fidelity witness. That is, by essentially neglecting the nonlinear terms in Eq. (7) we find that all states with Schmidt number bounded from above by  $r$  satisfy an inequality like Eq. (5). In particular taking  $Q_B(\alpha) = Q_A(-\alpha^*)$  from the hermitian part of the displacement operators, the left-hand

side becomes a fidelity-like witness with respect to a CV operator, representing the limiting case of an EPR state, with correlations given by  $\langle Q(\alpha) \otimes Q(\alpha') \rangle_{EPR} = \delta^{(2)}(\alpha' + \alpha^*)$ . For a detailed proof of these statements we refer to the End Matter.

**Applications.**— Let us illustrate how can we characterize the entanglement dimensionality of CV states with our method. First, let us consider a pure state in its Schmidt decomposed form  $|\psi\rangle = \sum_n \sqrt{\lambda_n} |nn\rangle$ , where  $\{\lambda_n\}$  converges for  $n \rightarrow \infty$ . First, let us consider the prototypical example of a symmetric two-mode squeezed thermal state [53, 54]

$$\varrho_{\text{TMST}}(\xi, \bar{n}) = U_\xi (\varrho(\bar{n}) \otimes \varrho(\bar{n})) U_\xi^\dagger, \quad (8)$$

where  $\varrho(\bar{n}) = \sum_{n=0}^{\infty} \frac{1}{\bar{n}+1} \left(\frac{\bar{n}}{\bar{n}+1}\right)^n |n\rangle\langle n|$  is a single-mode state with average particle number given by  $\bar{n}$  and  $U_\xi = e^{\xi(a_1^\dagger a_2^\dagger - a_1 a_2)}$  is the two-mode squeezing operator.

In this example, the Fock bases coincide with the Schmidt bases of target state and the state is symmetric and Gaussian. For such states, we can apply equivalently Eq. (5) or Eq. (7), with the two CVLOOs being  $Q(\alpha)$  and  $Q(-\alpha^*)$ , which makes the criteria equivalent to a fidelity witness with respect to the EPR state, which has been proven optimal, at least whenever the state is in a normal form [13]. As an alternative, for comparison, we can consider a typical truncation scheme applied in practical situations, where only a finite number  $d$  of Fock states are taken into account and the Schmidt number is characterized through the fidelity to the truncated two-mode squeezed state

$$|\psi_\xi^{(d)}\rangle = \sum_{n=0}^{d-1} \sqrt{N} \frac{(\tanh \xi)^n}{\cosh \xi} |nn\rangle, \quad (9)$$

where  $N$  is a renormalization factor due to the truncation.

The performance of the two criteria is shown in fig. 2 and we can observe that already a slight perturbation from the ideal pure state makes our criterion advantageous over the fidelity witness.

It is also worth emphasizing once more that in the case of symmetric Gaussian states the realignment criterion, which is weaker than Eq. (7), has been also compared to criteria based on the covariance matrix of quadrature observables and it was shown to also detect all such symmetric Gaussian states. See the SM [55] for more details on how to evaluate our criterion on Gaussian states. Still, the main features of this paradigmatic case actually apply in a far wider scenario. In fact, this example already clarifies that the main weakness of the finite-dimensionally-truncated fidelity method is that it can only detect states which are very close to the pure (truncated) target state, and is thus outperformed by our method in practical situations. In particular, one can easily see that the Gaussianity of the state is not important for our method. In fact, we can change the distribution of the Schmidt coefficients and still observe a similar behaviour.

For example, as an extremal case we can consider a flat distribution that is truncated to a finite (and large) point  $\lambda_n = 1/d$

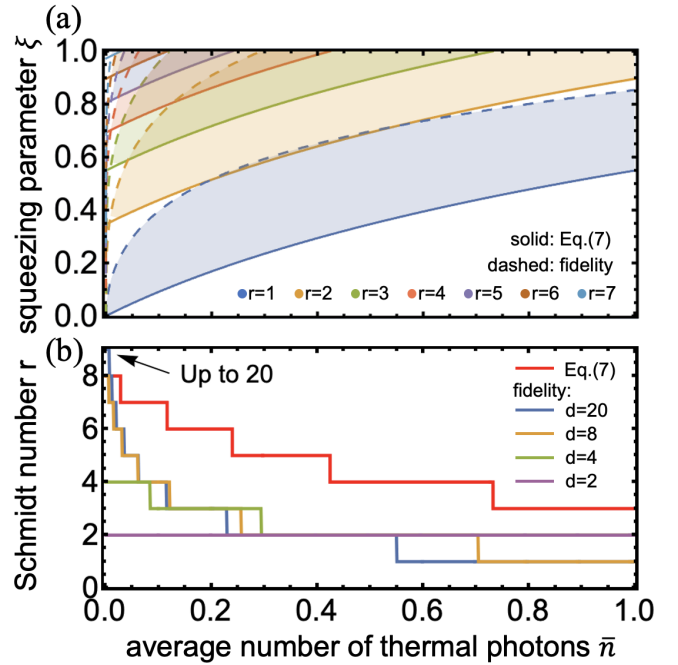


FIG. 2. Schmidt number bounds for the state Eq. (8). (a) Upper bounds on Schmidt number for  $r = 1$  to  $7$  (colour-coded) as functions of the average thermal photon number  $\bar{n}$  (horizontal axis) and squeezing parameter  $\xi$  (vertical axis). Solid lines correspond to the bounds from Eq. (7), which in this case coincide with Eq. (5), while dashed lines indicate those obtained via the finite-dimensional truncated fidelity witness (Eq. (2)) with optimal truncation dimensions. Points above each curve for a given  $r$  indicate Schmidt number of at least  $r + 1$ . The shaded region highlights where Eq. (7) outperforms the fidelity witness. Note also that the fidelity witness performance deteriorates rapidly as the state becomes increasingly mixed, as also shown in (b). (b) Schmidt number  $r$  versus average thermal photon number  $\bar{n}$  at fixed squeezing  $\xi = 1$ . Fidelity witnesses are shown for truncation dimensions  $d = 2, 4, 8, 20$ . Our criterion Eq. (7) strictly outperforms the fidelity witness even at  $d = 8$ . For very high truncation ( $d = 20$ ), the fidelity witness shows slight advantage only at low thermal noise.

for  $0 \leq n \leq d - 1$ , which would correspond to a finite-dimensional maximally entangled state. Even in this case, in which the fidelity to the corresponding (finite-dimensional) maximally entangled state is optimal and remains close to optimal also for states with symmetric noise, it can be still improved by a simple application of our method, but especially when the noise is asymmetric. That is considering the state

$$\varrho(p, \bar{n}) = p |\psi_+^d\rangle \langle \psi_+^d| + (1 - p)[\varrho(\bar{n}) \otimes \varrho(0)], \quad (10)$$

where  $|\psi_+^d\rangle = \frac{1}{\sqrt{d}} \sum_{n=0}^{d-1} |nn\rangle$  is the  $d$ -dimensional maximally entangled state, we obtain that our nonlinear criterion performs not worse or even slightly better than the fidelity witness with respect to  $|\psi_+^d\rangle$ . See fig. S2 in SM, where we considered  $d = 5$  and  $\bar{n} = 0.5$ , as well as a renormalization on the noise due to the truncated dimension.

Once again, here we applied the simple choice  $Q_B(\alpha) = Q_A(-\alpha^*)$  with the canonical  $Q(\alpha)$  given by the (normalized)

hermitian part of the displacement operator, and as a result obtained that the three criteria in Eqs. (5) and (7) perform identically. See also SM [55].

**Experimental implementation.**— Importantly, the methods we have proposed can find convenient experimental implementations, making them readily suited to state-of-the-art experiments. In hybrid CV-DV systems described by the Jaynes-Cummings Hamiltonian, the characteristic function of a bosonic mode can be measured through a two-level (*i.e.* a qubit) system [56, 57]. In particular, having available conditional displacements operations, namely displacements by  $D(\pm\alpha)$  depending on the state of the qubit, allows for the direct measurement of the real and imaginary parts of the mode's characteristic function through a measurement on the qubit [58–61]. Alternatively, similar protocols allows for the direct measurement of the Wigner function [62]. Both these type of measurements are nowadays routinely performed in trapped ions [59, 61, 63], cavity and circuit QED [60, 64–68], as well as in circuit quantum acoustodynamics [69, 70].

Although the previously-mentioned works focused on experimental techniques for the characterization of a single bosonic mode, extension of these methods to multi-mode systems is straightforward, both for the characteristic function [71] as well as for the Wigner function [72, 73]. With these available, to extract the quantities needed for our criteria, one needs to measure only a two-dimensional slice of the entire characteristic function (and thereby the correlations between CVLOOs  $Q(\alpha)$ ), which for two modes lives in a four-dimensional phase space. The role of the function  $f(\alpha)$  is to provide an additional phase-space transformation, that is not costly from a measurement point of view, since it corresponds to a post-processing of the data that allows us to improve the efficiency of the method. Note also that the characteristic function is complex valued and Hermitian  $\chi^*(\alpha) = \chi(-\alpha)$ , meaning that for a complete measurement only half of the  $\alpha$  complex space is sufficient. In most practical scenarios, it is sufficient to apply the function  $f$  only to mode B, which is what we also consider in our examples in the paper.

We now show how to implement these measurements using two-level ancillas within a hybrid CV-DV system. As sketched in Fig. 3, the method employs qubit  $\pi/2$  rotations with an adjustable phase  $\varphi$ :  $R_{\pi/2}(\varphi) = \begin{pmatrix} 1 & e^{i\varphi} \\ -e^{-i\varphi} & 1 \end{pmatrix}$  together with a conditional displacement  $U = |0\rangle\langle 0| \otimes \mathbb{1} + |1\rangle\langle 1| \otimes D(\alpha)$ , followed by an ancilla readout in the  $\sigma_z$  basis [71, 74]. We present two implementations for Eqs. (5) and (7). In fig. 3(a) (two-ancilla implementation), two readout qubits interact with the two CV modes and yield binary outcomes  $s^{(A)}$  and  $s^{(B)}$  per run. From the sample means, we obtain  $\hat{X}_\varrho(\alpha) = \frac{2}{\pi} (s^{(A)}s^{(B)} - \bar{s}^{(A)}\bar{s}^{(B)})$ , and  $\langle Q(\alpha) \rangle = \sqrt{\frac{2}{\pi}} \bar{s}$  for each mode. In fig. 3(b) (single-ancilla implementation), a single qubit is coupled sequentially to the two modes and measured in the  $\sigma_z$  basis. In this case,  $\langle Q_A(\alpha) \otimes Q_B(f(\alpha)) \rangle = \frac{2}{\pi} \langle \sigma_z \rangle$ . The nonlinear term  $\langle Q_A(\alpha) \rangle_\varrho \langle Q_B(f(\alpha)) \rangle_\varrho$  appearing in Eq. (6) can be accessed by setting one of the conditional displacements to the identity. Hence, the full quantity  $X_\varrho(\alpha)$  can like-

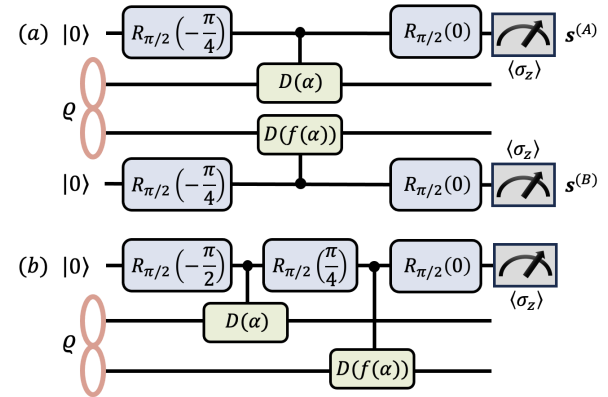


FIG. 3. Experimental implementation circuits of Eqs. (5) and (7). (a) Each CV mode of  $\varrho$  is coupled to its own ancillary readout qubit. Correlations in the  $Q(\alpha)$  CVLOOs can be computed from sequential readouts  $s = \{\pm 1\}$ . (b) Both CV modes interact sequentially with a single ancillary qubit.  $\langle Q_A(\alpha) \otimes Q_B(f(\alpha)) \rangle$  are then computed from the measured  $\langle \sigma_z \rangle$ .

wise be measured. See [72] for a typical experiment of similar scheme.

From the point of view of the state preparation, bipartite CV entangled states have been experimentally demonstrated in a variety of systems. Two-mode squeezed states have been extensively explored in optics and, more recently, also for the motional states of trapped ions [75], microwave fields [76, 77] and mechanical oscillators [78]. Besides these examples within the regime of Gaussian states, recent developments in the realization of universal gates and nonlinear dynamics across different platforms allowed for the demonstration of non-Gaussian entangled states. Apart from milestone optical experiments in the preparation of high-dimensional entangled states [79–89], entangled cats [72], coherent and Fock [73] states were demonstrated in circuit QED. These shows how the methods we have introduced in this work can find immediate application in a number of extremely relevant experimental platforms.

**Conclusions and outlook.**— In this work, we have extended the approach of quantifying entanglement via measurements of CVLOOs, by focusing on the characterization of the entanglement dimensionality by means of the Schmidt number. This is typically the main benchmark for characterizing the strength of entanglement for a number of applications that are typical of CV systems, ranging from quantum communication and cryptography [90, 91], to quantum computing [22] or foundational applications of entanglement [23]. In typical CV experiments, such as photonic setups, the most common approach certifies the entanglement dimensionality via a finite-dimensional truncation of the Hilbert space. Here, however, we have shown that applying the more natural approach of using inherently CV methods can lead to a better visibility of the entanglement dimensionality, that is more tolerant to noise than typical witnesses based on fidelities. In this sense,

our results are an important improvement of current literature and makes the characterization of entanglement dimensionality in CV system much more effective and readily implementable, significantly improving current approaches especially in realistic scenarios with noise. At the same time, we significantly improve the characterization of entanglement via CVLOOs, deriving new conditions that can also detect states invisible to the CCNR criterion investigated previously [13]. Our work also opens several further questions that deserve investigation, like the possibility to witness PPT entanglement of high-dimension in CV systems, which is still a challenging theoretical question, or the extension of our results to the genuinely multipartite case.

**Acknowledgements.**— This work is supported by the National Natural Science Foundation of China (Grants No. 12125402, No. 12534016, No. 12405005, No. 12505010, No. 12447157), Beijing Natural Science Foundation (Grant No. Z240007), and the Innovation Program for Quantum Science and Technology (No. 2024ZD0302401). S.L. acknowledges the China Postdoctoral Science Foundation (No. 2023M740119). J.G. acknowledges Postdoctoral Fellowship Program of CPSF (GZB20240027), and the China Postdoctoral Science Foundation (No. 2024M760072). MF was supported by the Swiss National Science Foundation Ambizione Grant No. 208886, and The Branco Weiss Fellowship – Society in Science, administered by the ETH Zürich. G.V. acknowledges financial support from the Austrian Science Fund (FWF) through the grants P 35810-N and P 36633-N (Stand-Alone). MH acknowledges funding from the Horizon-Europe research and innovation programme under grant agreement No 101070168 (HyperSpace) and the FFG through the Quantum Austria projects VANESSA-QC and MUSIQ.

**End Matter.**— We derive the first lower bound in Eq. (4) as follows. From the normalization condition  $s \text{tr}(\mathcal{O}(\alpha)\mathcal{O}(\beta)) = (2-s)\text{tr}(\tilde{\mathcal{O}}(\alpha)\tilde{\mathcal{O}}(\beta)) = \delta^{(2)}(\alpha-\beta)$  with  $0 < s < 2$ , we construct operators  $\mathcal{O}^{(1)}(\alpha) = \mathcal{O}(\alpha/\sqrt{s})$  and  $\tilde{\mathcal{O}}^{(1)}(\alpha) = \tilde{\mathcal{O}}(\alpha/\sqrt{2-s})$  that are normalized to 1. Introducing the angle parameter  $\theta = \arccos \sqrt{s/2}$ , we obtain

$$\int_{\mathbb{C}} \langle \mathcal{O}(\alpha) \otimes \tilde{\mathcal{O}}(\alpha) \rangle d^2\alpha = \frac{1}{2} \int_{\mathbb{C}} \langle \mathcal{O}^{(1)}(\alpha \cos \theta) \otimes \tilde{\mathcal{O}}^{(1)}(\alpha \sin \theta) \rangle d^2\alpha \quad (11)$$

When both  $\mathcal{O}^{(1)}$  and  $\tilde{\mathcal{O}}^{(1)}$  are displaced parity operators, the proof that the expression in Eq. (11) gives a lower bound to  $\|\mathcal{T}_A(\varrho)\|$  has been established in [48]. For the case where both operators are CVLOOs  $Q$ , the proof follows analogously.

Here we point out some short details on the transformations between various LOOs in CV systems. Given a discrete basis such as the Fock basis we can construct the observables  $g_\mu = |n\rangle\langle m|$  with  $\mu = (nm)$  being a compact label for both indices. These observables form a basis, that is also orthonormal as they satisfy  $\text{tr}(g_\mu^\dagger g_\nu) = \delta_{\mu\nu}$ . A change of basis, e.g., from a discrete to a continuous one, is done via an orthogonal kernel  $Q(\alpha) = \sum_\mu O_\mu(\alpha)g_\mu$  with  $O_\mu(\alpha) = \text{tr}(Q(\alpha)g_\mu^\dagger)$ . This transformation satisfies  $\sum_\mu O_\mu^\dagger(\alpha)O_\mu(\beta) = \delta^{(2)}(\alpha-\beta)$  and also

$\int_{\mathbb{C}} O_\mu^\dagger(\alpha)O_\nu(\alpha) d^2\alpha = \delta_{\mu\nu}$ . Analogous transformations allow to change between two continuous or two discrete bases. Now, we can give the explicit proof of the criterion in Eq. (7). This is based on the following Lemma, that provides a bound on the absolute value of the cross-covariances for pure states with a given Schmidt number.

**Lemma 1.** *Given any two CVLOOs  $Q_A(\alpha)$  and  $Q_B(\alpha)$ , for pure bipartite states  $|\psi_r\rangle$  with Schmidt rank not larger than  $r$ , the cross-covariances satisfy*

$$\int_{\mathbb{C}} |\Gamma_{\psi_r}(Q_A(\alpha), Q_B(\alpha))| d^2\alpha \leq r - \text{tr}([\text{tr}_b |\psi_r\rangle\langle\psi_r|]^2). \quad (12)$$

*Proof.*—Let us consider a pure Schmidt-rank- $r$  state in its Schmidt decomposition:  $|\psi_r\rangle = \sum_{n=0}^{r-1} \sqrt{\lambda_n} |nn\rangle$ , and let us take for each mode the discrete LOO  $g_{\mu=(nm)} = |n\rangle\langle m|$ . In this case, the nonzero cross-covariances of those observables form a (finite-dimensional)  $r^2 \times r^2$  matrix  $\Gamma_{\psi_r}(g_\mu^{(a)}, g_\nu^{(b)}) := (X_{\psi_r})_{\mu\nu} = \langle (g_\mu^{(a)})^\dagger \otimes g_\nu^{(b)} \rangle - \langle g_\mu^{(a)} \rangle \langle g_\nu^{(b)} \rangle$ , where  $\mu = (n, m)$  is a double-index with  $0 \leq n, m \leq (r-1)$ . Moreover, the following bound holds:  $\|X_{\psi_r}\| = \sum_{\mu=1}^{r^2} \Lambda_\mu = \sum_{n,m=0}^{r-1} \sqrt{\lambda_n \lambda_m} - \sum_n \lambda_n^2 \leq r - \sum_n \lambda_n^2 = r - \text{tr}([\text{tr}_b |\psi_r\rangle\langle\psi_r|]^2)$ , where we indicated with  $\Lambda_\mu$  the singular values of the matrix  $X_{\psi_r}$ . This bound is essentially due to  $\sum_{nm} \sqrt{\lambda_n \lambda_m} \leq r$ , plus the fact that the submatrix  $D_{nm} := \lambda_n \delta_{nm} - \lambda_n \lambda_m$  is positive semidefinite [39]. Now, in order to obtain Eq. (12) we have to make a change of CVLOOs from the (discrete) one that gives the singular value decomposition of  $X_{\psi_r}$ , which we indicate as  $\tilde{g}_\mu$ , to the (continuous) ones  $Q(\alpha)$ . Applying the transformation described earlier we get  $\int_{\mathbb{C}} |\Gamma_{\psi_r}(Q_A(\alpha), Q_B(\alpha))| d^2\alpha = \int_{\mathbb{C}} \left| \sum_\mu \text{tr}[Q_A(\alpha)\tilde{g}_\mu^{(a)}] \text{tr}[Q_B(\alpha)(\tilde{g}_\mu^{(b)})^\dagger] \Lambda_\mu \right| d^2\alpha \leq \sum_\mu \Lambda_\mu = \|X_{\psi_r}\|$ , where we have used the triangle inequality and the Cauchy–Schwarz inequality, exploiting the orthogonality of the basis changes.  $\square$

The CCNR criterion can be also expressed via correlations in a CVLOO. In particular, a similar reasoning as in the above proof can be made considering the cross-correlations  $(C_{\psi_r})_{\mu\nu} = \langle (g_\mu^{(a)})^\dagger \otimes g_\nu^{(b)} \rangle$ , that for a Schmidt-rank- $r$  pure state also form a  $r^2 \times r^2$  matrix with a bounded trace norm

$$\|C_{\psi_r}\| \leq r, \quad (13)$$

which gives a relation that can be similarly extended to all CVLOOs due to the orthogonality of the basis change. This condition is nothing but  $\|\mathcal{R}(\varrho)\| \leq r$  [13, 49]. One can then use the simple argument  $\langle Q_A(\alpha) \otimes Q_B(\alpha) \rangle_{\psi_r} \leq \|C_{\psi_r}\| \leq r$  valid for pure states and extend it to mixed states due to the linearity of the expression. This way one can then find a Schmidt-number condition as in Eq. (5) coming from the CCNR. A related argument can be found to bound the norm of the partially transposed matrix and obtain again an expression as in Eq. (5), this time with differently normalized observables [48], as we have also discussed earlier.

Based on Lemma 1 the proof of Eq. (7) follows. Once again, in this work we focus on specific CVLOOs, but the proof works in a more general scenario of two arbitrary bases for the two parties.

*Proof of Eq. (7)*—Let us consider a mixed bipartite state decomposed as  $\varrho = \sum_k p_k |\psi_k\rangle\langle\psi_k|$  where all the  $|\psi_k\rangle$  have Schmidt rank smaller or equal than a given  $r$ . Let us consider the functions

$$\begin{aligned}\mathcal{A}_\varrho(\alpha) &= (\mathcal{A}(Q_A(\alpha) \otimes \mathbb{1}))_\varrho^2 - \sum_k p_k (\mathcal{A}(Q_A(\alpha) \otimes \mathbb{1}))_{\psi_k}^2, \\ \mathcal{B}_\varrho(\alpha) &= (\mathcal{A}(\mathbb{1} \otimes Q_B(\alpha)))_\varrho^2 - \sum_k p_k (\mathcal{A}(\mathbb{1} \otimes Q_B(\alpha)))_{\psi_k}^2, \\ C_\varrho(\alpha) &= \Gamma_\varrho(Q_A(\alpha), Q_B(\alpha)) - \sum_k p_k \Gamma_{\psi_k}(Q_A(\alpha), Q_B(\alpha)).\end{aligned}\quad (14)$$

Now, we have that the inequality

$$\mathcal{A}_\varrho(\alpha) \mathcal{B}_\varrho(\alpha) \geq |C_\varrho(\alpha)|^2 \quad (15)$$

follows from the positivity of the matrix

$$\mathcal{A} := \begin{pmatrix} \mathcal{A}_\varrho(\alpha) & C_\varrho(\alpha) \\ C_\varrho(\alpha) & \mathcal{B}_\varrho(\alpha) \end{pmatrix} \geq 0, \quad (16)$$

which is in turn a consequence of the concavity and the positivity of covariance matrices.

This also implies that the following function is positive for all  $\alpha \in \mathbb{C}$  and  $t \in \mathbb{R}$ :

$$T_\varrho(\alpha, t) := \mathcal{A}_\varrho(\alpha) + 4t^2 \mathcal{B}_\varrho(\alpha) - 4|t| |C_\varrho(\alpha)| \geq 0, \quad (17)$$

and so is its integral over  $\alpha$ :  $\int_{\mathbb{C}} T_\varrho(\alpha, t) d^2\alpha \geq 0$ . Now, from the fact that for single modes it holds that  $S_L(\varrho) := 1 - \text{tr}(\varrho^2) = 1 - \int_{\mathbb{C}} \langle Q(\alpha) \rangle_\varrho^2 d^2\alpha$ , we can find the following relations

$$\begin{aligned}\int_{\mathbb{C}} \mathcal{A}_\varrho(\alpha) d^2\alpha &= S_L(Q_A) - \sum_k p_k S_L(\text{tr}_B(|\psi_k\rangle\langle\psi_k|)), \\ \int_{\mathbb{C}} \mathcal{B}_\varrho(\alpha) d^2\alpha &= S_L(Q_B) - \sum_k p_k S_L(\text{tr}_B(|\psi_k\rangle\langle\psi_k|)),\end{aligned}\quad (18)$$

and moreover we have that  $\int_{\mathbb{C}} |C_\varrho(\alpha)| d^2\alpha \geq \int_{\mathbb{C}} (|X_\varrho(\alpha)| - \sum_k p_k |X_{\psi_k}(\alpha)|) d^2\alpha$ , where now we introduced the notation  $\Gamma_\varrho(Q_A(\alpha), Q_B(\alpha)) := X_\varrho(\alpha)$  for simplicity. This last expression can be in turn bounded by using the inequality Eq. (12) from Lemma 1 as

$$\int_{\mathbb{C}} |C_\varrho(\alpha)| d^2\alpha \geq \int_{\mathbb{C}} |X_\varrho(\alpha)| d^2\alpha - r + \sum_k p_k \text{tr}([\text{tr}_B |\psi_k\rangle\langle\psi_k|]^2). \quad (19)$$

Substituting these relations into Eq. (17) and using  $S_L(\varrho) \geq 0$ , we find

$$\tilde{T}_\varrho(t) := S_L(Q_A) + 4t^2 S_L(Q_B) - 4|t| \left( \int_{\mathbb{C}} |X_\varrho(\alpha)| d^2\alpha - r + 1 \right) \geq 0, \quad (20)$$

which holds for all real values of  $t$ . Next, minimizing this function over all  $t \in \mathbb{R}$  we find

$$\int_{\mathbb{C}} |X_\varrho(\alpha)| d^2\alpha - \sqrt{S_L(Q_A) S_L(Q_B)} + 1 \leq r, \quad (21)$$

which results from the fact that the minimum of  $\tilde{T}_\varrho(t)$  is achieved for  $2|t| = (\int_{\mathbb{C}} |X_\varrho(\alpha)| d^2\alpha - r + 1) / S_L(Q_B)$  and is positive.  $\square$

Finally, we provide here explicit calculations for the circuits in fig. 3. Circuit (a): Each CV mode is coupled to its own ancilla, implementing a two-outcome POVM  $E_j = M_j^\dagger M_j$  with

$$\begin{aligned}M_0 &= \frac{1}{2} [\mathbb{1} - e^{i\pi/4} D(\alpha)], \\ M_1 &= \frac{1}{2} [-\mathbb{1} - e^{i\pi/4} D(\alpha)],\end{aligned}\quad (22)$$

Encoding the measurement outcome as  $\{\pm 1\}$  gives

$$\langle \sigma_z \rangle = \langle E_1 - E_0 \rangle = \frac{1}{2} \langle e^{-i\pi/4} D^\dagger(\alpha) + e^{i\pi/4} D(\alpha) \rangle. \quad (23)$$

Hence, for each mode,  $\langle Q(\alpha) \rangle = \sqrt{\frac{2}{\pi}} \langle \sigma_z \rangle = \sqrt{\frac{2}{\pi}} \bar{s}$  where  $\bar{s}$  is the sample mean of the binary outcomes. For two modes,  $\langle Q(\alpha) \otimes Q(f(\alpha)) \rangle = \frac{2}{\pi} \bar{s}^{(A)} \bar{s}^{(B)}$  and therefore

$$\hat{X}_\varrho^f(\alpha) = \frac{2}{\pi} (\bar{s}^{(A)} \bar{s}^{(B)} - \bar{s}^{(A)} \bar{s}^{(B)}). \quad (24)$$

Circuit (b): A single ancilla interacts sequentially with both modes. The setting again realizes a two-outcome POVM  $E_j = M_j^\dagger M_j$ , with

$$\begin{aligned}M_0 &= \frac{1}{2\sqrt{2}} [\mathbb{1} \otimes \mathbb{1} - ie^{i\pi/4} D_A \otimes \mathbb{1} - e^{-i\pi/4} \mathbb{1} \otimes D_B - iD_A \otimes D_B], \\ M_1 &= \frac{1}{2\sqrt{2}} [-\mathbb{1} \otimes \mathbb{1} + ie^{i\pi/4} D_A \otimes \mathbb{1} - e^{-i\pi/4} \mathbb{1} \otimes D_B - iD_A \otimes D_B],\end{aligned}\quad (25)$$

where  $D_{A,B}$  denotes  $D_A(\alpha)$  on mode  $A$  and  $D_B(f(\alpha))$  on mode  $B$ . It follows that

$$E_1 - E_0 = \frac{1}{4} [iD \otimes D + D \otimes D^\dagger + D^\dagger \otimes D - iD^\dagger \otimes D^\dagger]. \quad (26)$$

Therefore

$$\langle Q(\alpha) \otimes Q(f(\alpha)) \rangle = \frac{2}{\pi} \langle E_1 - E_0 \rangle = \frac{2}{\pi} \langle \sigma_z \rangle. \quad (27)$$

\* fadelm@phys.ethz.ch

† qiongyihe@pku.edu.cn

‡ marcus.huber@tuwien.ac.at

§ giuseppe.vitagliano@tuwien.ac.at

- [1] S. L. Braunstein and P. van Loock, Quantum information with continuous variables, Rev. Mod. Phys. **77**, 513 (2005).
- [2] C. Weedbrook, S. Pirandola, R. García-Patrón, N. J. Cerf, T. C. Ralph, J. H. Shapiro, and S. Lloyd, Gaussian quantum information, Rev. Mod. Phys. **84**, 621 (2012).
- [3] R. Simon, Peres-horodecki separability criterion for continuous variable systems, Phys. Rev. Lett. **84**, 2726 (2000).
- [4] L.-M. Duan, G. Giedke, J. I. Cirac, and P. Zoller, Inseparability criterion for continuous variable systems, Phys. Rev. Lett. **84**, 2722 (2000).
- [5] E. Shchukin and W. Vogel, Inseparability criteria for continuous bipartite quantum states, Phys. Rev. Lett. **95**, 230502 (2005).

[6] M. Hillery and M. S. Zubairy, Entanglement conditions for two-mode states, *Phys. Rev. Lett.* **96**, 050503 (2006).

[7] A. Miranowicz, M. Piani, P. Horodecki, and R. Horodecki, Inseparability criteria based on matrices of moments, *Phys. Rev. A* **80**, 052303 (2009).

[8] G. Giedke, B. Kraus, M. Lewenstein, and J. I. Cirac, Entanglement criteria for all bipartite gaussian states, *Phys. Rev. Lett.* **87**, 167904 (2001).

[9] P. van Loock and A. Furusawa, Detecting genuine multipartite continuous-variable entanglement, *Phys. Rev. A* **67**, 052315 (2003).

[10] P. Hyllus and J. Eisert, Optimal entanglement witnesses for continuous-variable systems, *New Journal of Physics* **8**, 51 (2006).

[11] D. Zhang, D. Barral, Y. Zhang, M. Xiao, and K. Bencheikh, Genuine tripartite non-gaussian entanglement, *Phys. Rev. Lett.* **130**, 093602 (2023).

[12] S. Yu and N.-l. Liu, Entanglement detection by local orthogonal observables, *Phys. Rev. Lett.* **95**, 150504 (2005).

[13] C. Zhang, S. Yu, Q. Chen, and C. H. Oh, Detecting and estimating continuous-variable entanglement by local orthogonal observables, *Phys. Rev. Lett.* **111**, 190501 (2013).

[14] G. Vidal, Entanglement monotones, *Journal of Modern Optics* **47**, 355 (2000).

[15] R. Horodecki, P. Horodecki, M. Horodecki, and K. Horodecki, Quantum entanglement, *Rev. Mod. Phys.* **81**, 865 (2009).

[16] J. Schneeloch, C. C. Tison, M. L. Fanto, P. M. Alsing, and G. A. Howland, Quantifying entanglement in a 68-billion-dimensional quantum state space, *Nature communications* **10**, 2785 (2019).

[17] B. M. Terhal and P. Horodecki, Schmidt number for density matrices, *Phys. Rev. A* **61**, 040301 (2000).

[18] M. Van den Nest, Universal quantum computation with little entanglement, *Phys. Rev. Lett.* **110**, 060504 (2013).

[19] M. Van den Nest, W. Dür, G. Vidal, and H. J. Briegel, Classical simulation versus universality in measurement-based quantum computation, *Phys. Rev. A* **75**, 012337 (2007).

[20] G. Vidal, Efficient classical simulation of slightly entangled quantum computations, *Phys. Rev. Lett.* **91**, 147902 (2003).

[21] S. Ecker, F. Bouchard, L. Bulla, F. Brandt, O. Kohout, F. Steinlechner, R. Fickler, M. Malik, Y. Guryanova, R. Ursin, and M. Huber, Overcoming noise in entanglement distribution, *Phys. Rev. X* **9**, 041042 (2019).

[22] P. Hrmo, B. Wilhelm, L. Gerster, M. W. van Mourik, M. Huber, R. Blatt, P. Schindler, T. Monz, and M. Ringbauer, Native qudit entanglement in a trapped ion quantum processor, *Nature Communications* **14**, 2242 (2023).

[23] M. Erhard, M. Krenn, and A. Zeilinger, Advances in high-dimensional quantum entanglement, *Nature Reviews Physics* **2**, 365 (2020).

[24] O. Lib, S. Liu, R. Shekel, Q. He, M. Huber, Y. Bromberg, and G. Vitagliano, Experimental certification of high-dimensional entanglement with randomized measurements, *Phys. Rev. Lett.* **134**, 210202 (2025).

[25] N. Herrera Valencia, V. Srivastav, M. Pivoluska, M. Huber, N. Friis, W. McCutcheon, and M. Malik, High-Dimensional Pixel Entanglement: Efficient Generation and Certification, *Quantum* **4**, 376 (2020).

[26] K.-C. Chang, M. C. Saruhan, X. Cheng, P. Erker, N. K. H. Li, A. Mueller, M. Spiropulu, M. D. Shaw, B. Korzh, M. Huber, and C. W. Wong, Experimental high-dimensional entanglement certification and quantum steering with time-energy measurements (2024), arXiv:2310.20694 [quant-ph].

[27] H. Yu, S. Sciara, M. Chemnitz, N. Montaut, B. Crockett, B. Fischer, R. Helsten, B. Wetzel, T. A. Goebel, R. G. Krämer, et al., Quantum key distribution implemented with d-level time-bin entangled photons, *Nature Communications* **16**, 171 (2025).

[28] B. Ndagano, H. Defienne, A. Lyons, I. Starshynov, F. Villa, S. Tisa, and D. Faccio, Imaging and certifying high-dimensional entanglement with a single-photon avalanche diode camera, *npj Quantum Information* **6**, 94 (2020).

[29] B. Courme, C. Vernière, P. Svihra, S. Gigan, A. Nomerotski, and H. Defienne, Quantifying high-dimensional spatial entanglement with a single-photon-sensitive time-stamping camera, *Opt. Lett.* **48**, 3439 (2023).

[30] H. Guo, N. Liu, Z. Li, R. Yang, H. Sun, K. Liu, and J. Gao, Generation of continuous-variable high-dimensional entanglement with three degrees of freedom and multiplexing quantum dense coding, *Photon. Res.* **10**, 2828 (2022).

[31] B. Courme, P. Cameron, D. Faccio, S. Gigan, and H. Defienne, Manipulation and certification of high-dimensional entanglement through a scattering medium, *PRX Quantum* **4**, 010308 (2023).

[32] S. Designolle, V. Srivastav, R. Uola, N. H. Valencia, W. McCutcheon, M. Malik, and N. Brunner, Genuine high-dimensional quantum steering, *Phys. Rev. Lett.* **126**, 200404 (2021).

[33] F. Shahandeh, J. Sperling, and W. Vogel, Operational gaussian schmidt-number witnesses, *Phys. Rev. A* **88**, 062323 (2013).

[34] J. Sperling and W. Vogel, Determination of the schmidt number, *Phys. Rev. A* **83**, 042315 (2011).

[35] N. Friis, G. Vitagliano, M. Malik, and M. Huber, Entanglement certification from theory to experiment, *Nat. Rev. Phys.* **1**, 72 (2019).

[36] Our results are formulated in a way that is immediately extendable to the more general scenario of  $N + M$  modes for the two parties, but we focus here on the  $(1 + 1)$  case for concreteness.

[37] A. I. Lvovsky and M. G. Raymer, Continuous-variable optical quantum-state tomography, *Rev. Mod. Phys.* **81**, 299 (2009).

[38] M. Weilenmann, B. Dive, D. Trillo, E. A. Aguilar, and M. Navascués, Entanglement Detection beyond Measuring Fidelities, *Phys. Rev. Lett.* **124**, 200502 (2020).

[39] S. Liu, M. Fadel, Q. He, M. Huber, and G. Vitagliano, Bounding entanglement dimensionality from the covariance matrix, *Quantum* **8**, 1236 (2024).

[40] M. Piani and C. E. Mora, Class of positive-partial-transpose bound entangled states associated with almost any set of pure entangled states, *Phys. Rev. A* **75**, 012305 (2007).

[41] M. Huber, L. Lami, C. Lancien, and A. Müller-Hermes, High-dimensional entanglement in states with positive partial transposition, *Phys. Rev. Lett.* **121**, 200503 (2018).

[42] R. Krebs and M. Gachechiladze, High schmidt number concentration in quantum bound entangled states, *Phys. Rev. Lett.* **132**, 220203 (2024).

[43] Note that there exist also discrete LOOs in CV systems, for example constructed from the Fock basis. However, in most of our discussion we focus on continuous LOOs, that fully characterize CV systems by means of quasi-probability distributions. See also End Matter and Supplemental Material [55].

[44] R. F. Bishop and A. Vourdas, Displaced and squeezed parity operator: Its role in classical mappings of quantum theories, *Phys. Rev. A* **50**, 4488 (1994).

[45] H. Moya-Cessa and P. L. Knight, Series representation of quantum-field quasiprobabilities, *Phys. Rev. A* **48**, 2479 (1993).

[46] T. Tilma, M. J. Everitt, J. H. Samson, W. J. Munro, and K. Nemoto, Wigner functions for arbitrary quantum systems, *Phys. Rev. Lett.* **117**, 180401 (2016).

[47] X. Qi and J. Hou, Nonlinear entanglement witnesses based on

continuous-variable local orthogonal observables for bipartite systems, *Quantum Information Processing* **15**, 741 (2016).

[48] S. Liu, J. Guo, Q. He, and M. Fadel, Quantum entanglement in phase space (2024), arXiv:2409.17891 [quant-ph].

[49] N. Johnston and D. W. Kribs, Duality of entanglement norms, *Houston J. Math.* **41**, 831 (2015).

[50] C. Eltschka and J. Siewert, Negativity as an estimator of entanglement dimension, *Phys. Rev. Lett.* **111**, 100503 (2013).

[51] S. Liu, Q. He, M. Huber, O. Gühne, and G. Vitagliano, Characterizing entanglement dimensionality from randomized measurements, *PRX Quantum* **4**, 020324 (2023).

[52] We omit the dependence of  $X_\varrho(\alpha)$  on the concrete basis to simplify the notation.

[53] P. Marian, T. A. Marian, and H. Scutaru, Bures distance as a measure of entanglement for two-mode squeezed thermal states, *Phys. Rev. A* **68**, 062309 (2003).

[54] S. H. Xiang, K. H. Song, W. Wen, and Z. G. Shi, Entanglement behaviors of two-mode squeezed thermal states in two different environments, *Eur. Phys. J. D* **62**, 289 (2011).

[55] See supplemental material for detailed proofs and examples.

[56] M. Wilkens and P. Meystre, Nonlinear atomic homodyne detection: A technique to detect macroscopic superpositions in a micromaser, *Phys. Rev. A* **43**, 3832 (1991).

[57] M. S. Kim, G. Antesberger, C. T. Bodendorf, and H. Walther, Scheme for direct observation of the wigner characteristic function in cavity qed, *Phys. Rev. A* **58**, R65 (1998).

[58] A. Asadian, C. Brukner, and P. Rabl, Probing Macroscopic Realism via Ramsey Correlation Measurements, *Physical Review Letters* **112**, 190402 (2014).

[59] K. Johnson, B. Neyenhuis, J. Mizrahi, J. Wong-Campos, and C. Monroe, Sensing Atomic Motion from the Zero Point to Room Temperature with Ultrafast Atom Interferometry, *Physical Review Letters* **115**, 213001 (2015).

[60] P. Campagne-Ibarcq, A. Eickbusch, S. Touzard, E. Zalys-Geller, N. E. Frattini, V. V. Sivak, P. Reinhold, S. Puri, S. Shankar, R. J. Schoelkopf, L. Frunzio, M. Mirrahimi, and M. H. Devoret, Quantum error correction of a qubit encoded in grid states of an oscillator, *Nature* **584**, 368 (2020).

[61] C. Flühmann and J. P. Home, Direct characteristic-function tomography of quantum states of the trapped-ion motional oscillator, *Phys. Rev. Lett.* **125**, 043602 (2020).

[62] L. G. Lutterbach and L. Davidovich, Method for direct measurement of the wigner function in cavity qed and ion traps, *Phys. Rev. Lett.* **78**, 2547 (1997).

[63] D. Leibfried, D. M. Meekhof, B. E. King, C. Monroe, W. M. Itano, and D. J. Wineland, Experimental Determination of the Motional Quantum State of a Trapped Atom, *Physical Review Letters* **77**, 4281 (1996).

[64] P. Bertet, A. Auffeves, P. Maioli, S. Osnaghi, T. Meunier, M. Brune, J. M. Raimond, and S. Haroche, Direct Measurement of the Wigner Function of a One-Photon Fock State in a Cavity, *Physical Review Letters* **89**, 200402 (2002).

[65] B. Vlastakis, G. Kirchmair, Z. Leghtas, S. E. Nigg, L. Frunzio, S. M. Girvin, M. Mirrahimi, M. H. Devoret, and R. J. Schoelkopf, Deterministically Encoding Quantum Information Using 100-Photon Schrödinger Cat States, *Science* **342**, 607 (2013).

[66] A. Eickbusch, V. Sivak, A. Z. Ding, S. S. Elder, S. R. Jha, J. Venkatraman, B. Royer, S. M. Girvin, R. J. Schoelkopf, and M. H. Devoret, Fast universal control of an oscillator with weak dispersive coupling to a qubit, *Nature Physics* **18**, 1464 (2022).

[67] A. A. Diringer, E. Blumenthal, A. Grinberg, L. Jiang, and S. Hacohen-Gourgy, Conditional-not Displacement: Fast Multioscillator Control with a Single Qubit, *Physical Review X* **14**, 011055 (2024).

[68] F. Valadares, N.-N. Huang, K. T. N. Chu, A. Dorogov, W. Chua, L. Kong, P. Song, and Y. Y. Gao, On-demand transposition across light-matter interaction regimes in bosonic cQED, *Nature Communications* **15**, 5816 (2024).

[69] K. J. Satzinger, Y. P. Zhong, H.-S. Chang, G. A. Peairs, A. Binenfai, M.-H. Chou, A. Y. Cleland, C. R. Conner, E. Dumur, J. Grebel, I. Gutierrez, B. H. November, R. G. Povey, S. J. Whiteley, D. D. Awschalom, D. I. Schuster, and A. N. Cleland, Quantum control of surface acoustic-wave phonons, *Nature* **563**, 661 (2018).

[70] U. Von Lüpke, Y. Yang, M. Bild, L. Michaud, M. Fadel, and Y. Chu, Parity measurement in the strong dispersive regime of circuit quantum acoustodynamics, *Nature Physics* **18**, 794 (2022).

[71] L. H. Zaw, Certifiable lower bounds of wigner negativity volume and non-gaussian entanglement with conditional displacement gates, *Phys. Rev. Lett.* **133**, 050201 (2024).

[72] C. Wang, Y. Y. Gao, P. Reinhold, and et. al., A schrödinger cat living in two boxes, *Science* **352**, 1087 (2016).

[73] Y. Y. Gao, B. J. Lester, K. S. Chou, L. Frunzio, M. H. Devoret, L. Jiang, S. M. Girvin, and R. J. Schoelkopf, Entanglement of bosonic modes through an engineered exchange interaction, *Nature* **566**, 509 (2019).

[74] A. Asadian, P. Erker, M. Huber, and C. Klöckl, Heisenberg-weyl observables: Bloch vectors in phase space, *Phys. Rev. A* **94**, 010301 (2016).

[75] J. Metzner, A. Quinn, S. Brudney, I. D. Moore, S. C. Burd, D. J. Wineland, and D. T. C. Allcock, Two-mode squeezing and  $su(1,1)$  interferometry with trapped ions, *Phys. Rev. A* **110**, 022613 (2024).

[76] C. Eichler, D. Bozyigit, C. Lang, M. Baur, L. Steffen, J. M. Fink, S. Filipp, and A. Wallraff, Observation of two-mode squeezing in the microwave frequency domain, *Phys. Rev. Lett.* **107**, 113601 (2011).

[77] E. Flurin, N. Roch, F. Mallet, M. H. Devoret, and B. Huard, Generating entangled microwave radiation over two transmission lines, *Phys. Rev. Lett.* **109**, 183901 (2012).

[78] H. F. H. Cheung, Y. S. Patil, L. Chang, S. Chakram, and M. Vengalattore, Nonlinear phonon interferometry at the heisenberg limit (2016), arXiv:1601.02324 [quant-ph].

[79] M. Krenn, M. Huber, R. Fickler, R. Lapkiewicz, S. Ramelow, and A. Zeilinger, Generation and confirmation of a  $(100 \times 100)$ -dimensional entangled quantum system, *Proceedings of the National Academy of Sciences* **111**, 6243 (2014).

[80] A. C. Dada, J. Leach, G. S. Buller, M. J. Padgett, and E. Andersson, Experimental high-dimensional two-photon entanglement and violations of generalized bell inequalities, *Nature Physics* **7**, 677 (2011).

[81] C. Schaeff, R. Polster, M. Huber, S. Ramelow, and A. Zeilinger, Experimental access to higher-dimensional entangled quantum systems using integrated optics, *Optica* **2**, 523 (2015).

[82] A. Martin, T. Guerreiro, A. Tiranov, S. Designolle, F. Fröwis, N. Brunner, M. Huber, and N. Gisin, Quantifying photonic high-dimensional entanglement, *Phys. Rev. Lett.* **118**, 110501 (2017).

[83] M. Malik, M. Erhard, M. Huber, M. Krenn, R. Fickler, and A. Zeilinger, Multi-photon entanglement in high dimensions, *Nature Photonics* **10**, 248 (2016).

[84] X.-M. Hu, W.-B. Xing, B.-H. Liu, Y.-F. Huang, C.-F. Li, G.-C. Guo, P. Erker, and M. Huber, Efficient generation of high-dimensional entanglement through multipath down-conversion, *Phys. Rev. Lett.* **125**, 090503 (2020).

[85] J. Huang, J. Mao, X. Li, J. Yuan, Y. Zheng, C. Zhai, T. Dai,

Z. Fu, J. Bao, Y. Yang, et al., Integrated optical entangled quantum vortex emitters, *Nature Photonics* **19**, 471 (2025).

[86] H. Mahmudlu, R. Johanning, A. Van Rees, A. Khodadad Kashi, J. P. Epping, R. Haldar, K.-J. Boller, and M. Kues, Fully on-chip photonic turnkey quantum source for entangled qubit/qudit state generation, *Nature Photonics* **17**, 518 (2023).

[87] A. Raymond, A. Zecchetto, J. Palomo, M. Morassi, A. Lemaître, F. Raineri, M. I. Amanti, S. Ducci, and F. Baboux, Tunable generation of spatial entanglement in nonlinear waveguide arrays, *Phys. Rev. Lett.* **133**, 233602 (2024).

[88] M. Erhard, M. Malik, M. Krenn, and A. Zeilinger, Experimental Greenberger–Horne–Zeilinger entanglement beyond qubits, *Nature Photonics* **12**, 759 (2018).

[89] J. Wang, S. Paesani, Y. Ding, R. Santagati, P. Skrzypczyk, A. Salavrakos, J. Tura, R. Augusiak, L. Mančinska, D. Bacco, et al., Multidimensional quantum entanglement with large-scale integrated optics, *Science* **360**, 285 (2018).

[90] L. Bulla, M. Pivoluska, K. Hjorth, O. Kohout, J. Lang, S. Ecker, S. P. Neumann, J. Bittermann, R. Kindler, M. Huber, M. Bohmann, and R. Ursin, Nonlocal temporal interferometry for highly resilient free-space quantum communication, *Phys. Rev. X* **13**, 021001 (2023).

[91] L. Bulla, K. Hjorth, O. Kohout, J. Lang, S. Ecker, S. P. Neumann, J. Bittermann, R. Kindler, M. Huber, M. Bohmann, R. Ursin, and M. Pivoluska, Distribution of genuine high-dimensional entanglement over 10.2 km of noisy metropolitan atmosphere, *Phys. Rev. A* **107**, L050402 (2023).

[92] K. E. Cahill and R. J. Glauber, Ordered expansions in boson amplitude operators, *Phys. Rev.* **177**, 1857 (1969).

## Supplemental Material

### Basic quantities for CV system

A discrete basis for the state space of each mode is given by the Fock basis  $|n\rangle$ , i.e., the eigenvectors of the number operator  $\hat{N} = \hat{a}^\dagger \hat{a}$  and every operator can be expanded as

$$Q = \sum_{nm} Q_{nm} |n\rangle\langle m| := \sum_{nm} Q_{nm} g_{nm}, \quad (\text{S1})$$

where  $Q_{nm} = \text{tr}(Q g_{nm}^\dagger)$ . A similar relation holds for any other complete basis, which we can call a CVLOO.

In particular, a different (and equally complete) description of quantum states and operators can be given in terms of the characteristic function, which is defined as [2]

$$\chi_\varrho(\alpha) = \text{tr}(\varrho D(\alpha)). \quad (\text{S2})$$

Thus in this case the (non-Hermitian) basis of the operators is given by the Weyl displacements, which satisfy [92]

$$\text{tr}(D^\dagger(\alpha) D(\beta)) = \pi \delta^{(2)}(\alpha - \beta) \quad (\text{S3})$$

From this representation we can also obtain the two-mode Wigner function as [44–46]

$$W_\varrho(\alpha) = \left(\frac{2}{\pi}\right)^2 \text{tr}(\varrho D(\alpha) \hat{P} D^\dagger(\alpha)), \quad (\text{S4})$$

where  $\hat{P} = (-1)^{\hat{N}}$  is the parity operator. This also suggests a method to directly experimentally measure the joint Wigner function at a point in phase space and also enlightens that in this case the CVLOO is given by displaced parity operators.

We can also define Hermitian versions of these CVLOOs, in particular

$$Q(\alpha) = \frac{1+i}{2\sqrt{\pi}} D(\alpha) + \frac{1-i}{2\sqrt{\pi}} D^\dagger(\alpha), \quad (\text{S5})$$

which then satisfies

$$\text{tr}(Q(\alpha) Q(\beta)) = \delta^{(2)}(\alpha - \beta) \quad (\text{S6})$$

A change of basis, e.g., from a discrete to a continuous one, is done via an orthogonal kernel

$$Q(\alpha) = \sum_\mu O_\mu(\alpha) g_\mu \quad \text{with} \quad O_\mu(\alpha) = \text{tr}(Q(\alpha) g_\mu^\dagger). \quad (\text{S7})$$

This transformation satisfies

$$\sum_\mu O_\mu^\dagger(\alpha) O_\mu(\beta) = \delta^{(2)}(\alpha - \beta), \quad (\text{S8})$$

and also  $\int_{\mathbb{C}} O_\mu^\dagger(\alpha) O_\nu(\alpha) d^2\alpha = \delta_{\mu\nu}$ . In particular, the change of basis from the (discrete) Fock basis to the (continuous) displacement operators can be obtained from the characteristic function of the operator  $|m\rangle\langle n|$ , which is given by [92]

$$\text{tr}(D(\alpha) g_{nm}) := \langle n | D(\alpha) | m \rangle = \begin{cases} e^{-|\alpha|^2/2} \sqrt{\frac{m!}{n!}} \alpha^{n-m} L_m^{(n-m)}(|\alpha|^2), & n \geq m, \\ e^{-|\alpha|^2/2} \sqrt{\frac{n!}{m!}} (\alpha^*)^{m-n} L_n^{(m-n)}(|\alpha|^2), & n < m. \end{cases} \quad (\text{S9})$$

where  $L_q^{(p)}$  is a Laguerre polynomial.

From a CVLOO we can also express the purity of a single-particle CV state as

$$\text{tr}(\varrho^2) = \int_{\mathbb{C}} \langle Q(\alpha) \rangle_\varrho^2 d^2\alpha, \quad (\text{S10})$$

and defining the variance of an operator  $A$  on a quantum state  $\varrho$  as  $(\Delta A)_{\varrho}^2 := \langle A^2 \rangle_{\varrho} - \langle A \rangle_{\varrho}^2$  we have

$$\int_{\mathbb{C}} [(\Delta Q(\alpha))_{\varrho_1}^2 - (\Delta Q(\alpha))_{\varrho_2}^2] d^2\alpha = \text{tr}(\varrho_2^2) - \text{tr}(\varrho_1^2) = S_L(\varrho_1) - S_L(\varrho_2) \quad (\text{S11})$$

where we defined the linear entropy as  $S_L(\varrho) := 1 - \text{tr}(\varrho^2)$ . Note that the normalization of the quantum state translates into

$$\text{tr}(\varrho) = \chi_{\varrho}(0) = \int_{\mathbb{C}} W_{\varrho}(\alpha) d^2\alpha = 1. \quad (\text{S12})$$

For a two (or more)-mode system we can compactify the notation by considering the vector of quadratures  $\mathbf{r} = (x_1, p_1, x_2, p_2)$ , given by

$$\hat{x}_j = \hat{a}_j + \hat{a}_j^\dagger \quad \hat{p}_j = i(\hat{a}_j^\dagger - \hat{a}_j), \quad (\text{S13})$$

that satisfy canonical commutation relations in the form  $[\hat{r}_j, \hat{r}_k] = 2i\varrho_{jk}\hat{1}$ , where we introduced the symplectic form  $\boldsymbol{\Omega} = (\begin{smallmatrix} 0 & 1 \\ -1 & 0 \end{smallmatrix}) \oplus (\begin{smallmatrix} 0 & 1 \\ -1 & 0 \end{smallmatrix})$ .

Weyl displacements can be then also expressed in terms of a real vector  $\mathbf{y} \in \mathbb{R}^2$

$$D(\mathbf{y}) = \exp(i\hat{\mathbf{r}}^\top \boldsymbol{\Omega} \mathbf{y}), \quad (\text{S14})$$

where we emphasized with a hat that the vector of quadratures is an operator vector. A particularly important class of states is given by Gaussian states, that have a characteristic function which can be expressed in the form [2]

$$\chi_{\varrho}(\mathbf{y}) = \text{tr}(\varrho D(\mathbf{y})) = \exp\left(-\frac{1}{2}\mathbf{y}^\top \boldsymbol{\Omega} \Gamma \boldsymbol{\Omega}^\top \mathbf{y} - i\mathbf{d}^\top \boldsymbol{\Omega}^\top \mathbf{y}\right), \quad (\text{S15})$$

where

$$\begin{aligned} \mathbf{d} &= (\langle x_1 \rangle_{\varrho}, \langle p_1 \rangle_{\varrho}, \langle x_2 \rangle_{\varrho}, \langle p_2 \rangle_{\varrho}), \\ [\Gamma]_{jk} &= \frac{1}{2}\langle \hat{r}_j \hat{r}_k + \hat{r}_k \hat{r}_j \rangle_{\varrho} - \langle \hat{r}_j \rangle_{\varrho} \langle \hat{r}_k \rangle_{\varrho}, \end{aligned} \quad (\text{S16})$$

are the mean vector and the covariance matrix respectively.

From this representation we can also obtain the joint Wigner function via Fourier transform as

$$W(\mathbf{r}) = \int_{\mathbb{R}^4} \frac{d^4\mathbf{y}}{(2\pi)^4} \exp(-i\mathbf{r}^\top \boldsymbol{\Omega} \mathbf{y}) \chi(\mathbf{y}), \quad (\text{S17})$$

where note that now  $\mathbf{r}$  is a vector of real numbers, not of quantum operators.

### Further details on the states detected

#### Gaussian states

As a prototypical example we can consider the one-parameter family of two-mode squeezed vacuum states, which are written in Fock basis as

$$|\psi\rangle = \sum_n \sqrt{\lambda_n} |nn\rangle, \quad (\text{S18})$$

with Schmidt coefficients given by:

$$\lambda_n = \frac{(\tanh \xi)^{2n}}{(\cosh \xi)^2}, \quad (\text{S19})$$

and  $\xi$  being the squeezing parameter. In particular, the Fock bases are the Schmidt bases and the entanglement dimensionality should be ideally infinity.

The covariance matrix of such a state is given by

$$\Gamma_{\psi_\xi} = \begin{pmatrix} \cosh(2\xi) & 0 & \sinh(2\xi) & 0 \\ 0 & \cosh(2\xi) & 0 & -\sinh(2\xi) \\ \sinh(2\xi) & 0 & \cosh(2\xi) & 0 \\ 0 & -\sinh(2\xi) & 0 & \cosh(2\xi) \end{pmatrix}, \quad (\text{S20})$$

and correspondingly, we can write its Wigner function and characteristic function via Eqs. (S15) and (S17). To apply our methods, we take  $f(\alpha) = -\alpha^*$ , that essentially translates Eq. (7), as well as Eq. (5) into:

$$\int_{\mathbb{C}} \langle Q_A(\alpha) \otimes Q_B(f(\alpha)) \rangle d^2\alpha \leq r, \quad (\text{S21})$$

Then, we use that

$$\begin{aligned} \int_{\mathbb{C}} X_{\psi_\xi}(\alpha) d^2\alpha &= \int_{\mathbb{C}} \Gamma_\varrho(Q_A(\alpha), Q_B(f(\alpha))) d^2\alpha = -\frac{2\nu(\nu+1)}{(\nu-1)(\nu^2+1)}, \\ \int_{\mathbb{C}} \langle Q_A(\alpha) \otimes \mathbb{1} \rangle^2 d^2\alpha &= \int_{\mathbb{C}} \langle \mathbb{1} \otimes Q_B(f(\alpha)) \rangle^2 d^2\alpha = \frac{1-\nu^2}{1+\nu^2}, \end{aligned} \quad (\text{S22})$$

where we have introduced the parameter  $\nu$  that is such that  $e^{2\xi} = \frac{1+\nu}{1-\nu}$ . From this, we can see that the Schmidt number detected by our method is

$$r \geq \frac{1+\nu}{1-\nu} = e^{2\xi}, \quad (\text{S23})$$

which is a finite number. Thus, it seems that for the ideal pure state our method is not fully optimal, as the ideal entanglement dimensionality would be infinite.

However, let us now compare our method with other criteria in practical circumstances. First we consider a mixture of the two-mode squeezed state with single-mode thermal noise as

$$\varrho(p) = p |\psi_\xi\rangle\langle\psi_\xi| + (1-p)[\varrho(\bar{n}) \otimes \varrho(\bar{n})], \quad (\text{S24})$$

where  $\varrho(\bar{n}) = \sum_{n=0}^{\infty} \frac{1}{\bar{n}+1} \left(\frac{\bar{n}}{\bar{n}+1}\right)^n |n\rangle\langle n|$  is a single-mode state with average particle number given by  $\bar{n}$  and  $0 \leq p \leq 1$  is a probability. Applying once again our method with the choice  $f(\alpha) = -\alpha^*$ , i.e., reduced to Eq. (S21), we get the condition

$$\frac{1-p}{2\bar{n}+1} + e^{2\xi} p \leq r, \quad (\text{S25})$$

where once again  $r$  is a given Schmidt number. Let us now compare this with the entanglement dimensionality detected by the fidelity witness in a typical truncation scheme to a finite-dimensional state, which simulates typical measurements. Thus, we truncate the system's dimension by only preserving the first  $d$  Fock states for each subsystem and then renormalize the state. We then take as the target state for the fidelity witness the truncated two-mode squeezed state, that reads

$$|\psi_\xi^{(d)}\rangle = \sum_{n=0}^{d-1} \sqrt{N} \frac{(\tanh \xi)^n}{\cosh \xi} |nn\rangle, \quad (\text{S26})$$

where  $N$  is the renormalization factor. As a result, we obtain that our method outperforms the truncated-fidelity witness, apart when the state is extremely close to be fully pure. See fig. S1.

### Non-Gaussian states

To show how our method works beyond the case of Gaussian states, let us consider a state that has a flat sequence of Schmidt coefficients, and let us truncate it to a  $d$ -dimensional maximally entangled state  $|\psi_+^d\rangle = \frac{1}{\sqrt{d}} \sum_{i=0}^{d-1} |ii\rangle$ . Clearly, such a pure state is detected optimally by the fidelity to itself. However, such a fidelity witness is also quite sensitive to noise, and we can see in the following that actually our method outperforms it. To show this, let us consider this maximally entangled state mixed with symmetric thermal noise:

$$\varrho(p, \bar{n}) = p |\psi_+^d\rangle\langle\psi_+^d| + (1-p)[\varrho(\bar{n}) \otimes \varrho(\bar{n})] \quad (\text{S27})$$

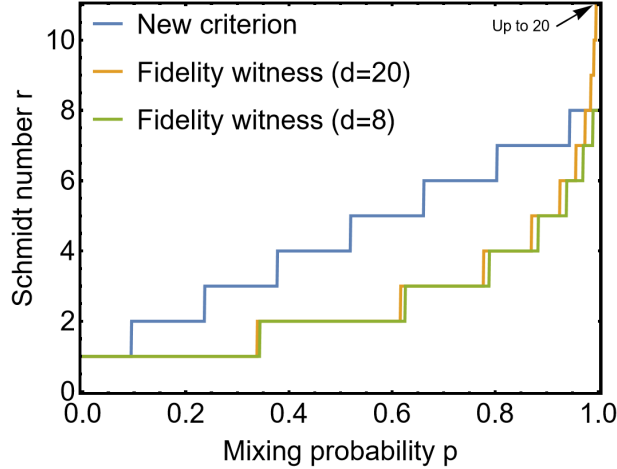


FIG. S1. We test both the CV (Eq. (7)) and DV (Eq. (2)) criteria using  $\varrho(p)$  in Eq. (S24) with  $\xi = 1.0, \bar{n} = 1.0$ . When truncating the state to  $d = 20$ , although the fidelity witness can certify Schmidt number  $r = 20$  when the state is very pure, it underperforms the CV criterion for most of the mixing probability  $p$ .

where  $\varrho(\bar{n})$  is a single-mode thermal state with mean photon number  $\bar{n}$ .

First, we compute the characteristic function of  $|\psi_+^d\rangle$ , that is

$$\chi_{\psi_+^d}(\alpha_1, \alpha_2) = \frac{1}{d} \sum_{i,j=0}^{d-1} \langle i | D(\alpha_1) | j \rangle \langle i | D(\alpha_2) | j \rangle = \frac{e^{-(|\alpha_1|^2 + |\alpha_2|^2)/2}}{d} \sum_{i,j=0}^{d-1} \begin{cases} \frac{j!}{i!} (\alpha_1 \alpha_2)^{i-j} L_j^{(i-j)}(|\alpha_1|^2) L_j^{(i-j)}(|\alpha_2|^2), & i \geq j, \\ \frac{i!}{j!} (\alpha_1^* \alpha_2^*)^{j-i} L_i^{(j-i)}(|\alpha_1|^2) L_i^{(j-i)}(|\alpha_2|^2), & i < j. \end{cases} \quad (S28)$$

Since it is symmetric  $\chi_{\psi_+^d}(-\alpha_1, -\alpha_2) = \chi_{\psi_+^d}(\alpha_1, \alpha_2)$  and  $Q(\alpha) = \frac{1+i}{2\sqrt{\pi}} D(\alpha) + \frac{1-i}{2\sqrt{\pi}} D^\dagger(\alpha)$ , we then have

$$\langle Q(\alpha_1) \otimes Q(\alpha_2) \rangle_{\psi_+^d} = \frac{1}{\pi} \chi_{\psi_+^d}(\alpha_1, -\alpha_2) \quad (S29)$$

Selecting  $\alpha_1 = -\alpha^*$  and  $\alpha_2 = \alpha$ , we obtain

$$\langle Q(-\alpha^*) \otimes Q(\alpha) \rangle_{\psi_+^d} = \frac{e^{-|\alpha|^2}}{\pi d} \sum_{i,j=0}^{d-1} \begin{cases} \frac{j!}{i!} (|\alpha|^2)^{i-j} [L_j^{(i-j)}(|\alpha|^2)]^2, & i \geq j, \\ \frac{i!}{j!} (|\alpha|^2)^{j-i} [L_i^{(j-i)}(|\alpha|^2)]^2, & i < j. \end{cases} \quad (S30)$$

The characteristic function of single-mode thermal noise is  $\chi_{\varrho(\bar{n})}(\alpha_x, \alpha_y) = e^{-\frac{(2\bar{n}+1)(\alpha_x^2 + \alpha_y^2)}{2}}$ . Therefore,  $\langle Q(-\alpha^*) \otimes Q(\alpha) \rangle_{\rho}$  is non-negative.

Switching to polar coordinates,  $d^2\alpha = r dr d\theta$  with  $\int_0^{2\pi} d\theta = 2\pi$ , we have

$$\int_{\mathbb{C}} \langle Q(-\alpha^*) \otimes Q(\alpha) \rangle_{\psi_+^d} d^2\alpha = \frac{1}{d} \sum_{i,j=0}^{d-1} \int_0^\infty x^{|i-j|} e^{-x} dx \times \begin{cases} \frac{j!}{i!} [L_j^{(i-j)}(x)]^2, & i \geq j \\ \frac{i!}{j!} [L_i^{(j-i)}(x)]^2, & i < j \end{cases} \quad (S31)$$

where  $x = r^2$ . Using the orthogonality relation for the associated Laguerre polynomials,  $\int_0^\infty e^{-x} x^k L_n^k(x) L_m^k(x) dx = \frac{(n+k)!}{n!} \delta_{mn}$ , we have

$$\begin{aligned} \int_{\mathbb{C}} \langle Q(-\alpha^*, \alpha) \rangle_{\psi_+^d} d^2\alpha &= \frac{1}{d} \sum_{i,j=0}^{d-1} \begin{cases} \frac{j!}{i!} \frac{i!}{j!}, & i \geq j \\ \frac{i!}{j!} \frac{j!}{i!}, & i < j \end{cases} \\ &= d \end{aligned} \quad (S32)$$

Similarly, for the product of two thermal states,

$$\int_{\mathbb{C}} \langle Q(-\alpha^*) \otimes Q(\alpha) \rangle_{[\varrho(\bar{n}) \otimes \varrho(\bar{n})]} = \frac{1}{2\bar{n} + 1}. \quad (S33)$$

Therefore the threshold condition becomes  $r \geq dp + (1-p)\frac{1}{2\bar{n}+1}$ .

The single-mode thermal state is  $\varrho(\bar{n}) = \sum_{n=0}^{\infty} p_n |n\rangle\langle n|$  where  $p_n = \frac{(\frac{\bar{n}}{1+\bar{n}})^n}{1+\bar{n}}$ . The fidelity with the  $d$ -dimensional maximally entangled state  $|\psi_+^d\rangle$  is

$$\begin{aligned}
 F\left(|\psi_+^d\rangle\langle\psi_+^d|, \varrho(\bar{n}) \otimes \varrho(\bar{n})\right) &= \sum_{n,m=0}^{\infty} p_n p_m \langle\psi_+^d|n, m\rangle\langle n, m|\psi_+^d\rangle \\
 &= \frac{1}{d} \sum_{n=0}^{d-1} p_n^2 \\
 &= \frac{1}{d(1+\bar{n})^2} \sum_{n=0}^{d-1} \left(\frac{\bar{n}}{1+\bar{n}}\right)^{2n} \\
 &= \frac{1 - \left(\frac{\bar{n}}{1+\bar{n}}\right)^{2d}}{d(1+2\bar{n})}
 \end{aligned} \tag{S34}$$

The fidelity witness  $F \leq \frac{r}{d}$  gives  $r \geq dp + (1-p)\frac{1 - \left(\frac{\bar{n}}{1+\bar{n}}\right)^{2d}}{2\bar{n}+1}$ . This threshold is strictly worse than  $dp + (1-p)\frac{1}{2\bar{n}+1}$  obtained from our method, even though the difference is very small and practically negligible.

However, when we consider asymmetric thermal noise as:

$$\varrho(p, \bar{n}) = p |\psi_+^d\rangle\langle\psi_+^d| + (1-p)[\varrho(\bar{n}) \otimes \varrho(0)], \tag{S35}$$

we obtain that our nonlinear criterion performs better than the fidelity witness with respect to  $|\psi_+^d\rangle$  more obviously. See fig. S2. Here we considered  $d = 5$  and  $\bar{n} = 0.5$  and a renormalization due to the truncated dimension.

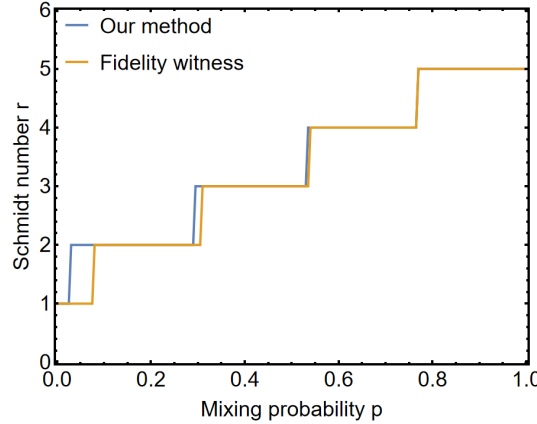


FIG. S2. Certified Schmidt number  $r$  with respect to the mixing probability  $p$  in Eq. (S35), using our method Eq. (7) and the fidelity witness Eq. (2).